# Heat Transfer and Fluid Flow Characteristics for Newtonian and Non-Newtonian Fluids in a Tube-in-Tube Helical Coil Heat Exchanger

Naveen Kushwaha[1], Tara Chand Kumawat[1], Krishna Deo Prasad Nigam[2], Vimal Kumar[1,*]
[1]Department of Chemical Engineering, Indian Institute of Technology Roorkee,
Uttarakhand – 247667, India
[2]Department of Chemical Engineering, Indian Institute of Technology Delhi,
Delhi–247667, India

**Abstract**

In the present work, heat transfer and fluid flow characteristics for both Newtonian and non-Newtonian fluids in tube-in-tube helical coil (TTHC) heat exchangers have been investigated numerically. The various TTHC heat exchanger configurations studied are: 1) parallel flow with and without baffles, and 2) counter flow with and without baffles. The power law index ($n$) and Dean Number ($N_{De}$) are varied from 0.5 to 1.25 and 50 to 500, respectively. Further, two different models have been proposed to predict the friction factor and Nusselt number in TTHC. It is observed that the $f$ and $Nu$ in TTHC heat exchanger with baffles in the annulus is higher as compared to TTHC heat exchanger without baffles. It is also found that at low Prandtl number the baffles have significant influence on heat transfer, while at high Prandtl number flow configuration has high significance.

***Keywords***: Tube-in-tube helical heat exchanger, computational fluid dynamics, heat transfer, friction factor, power law fluids, effectiveness-NTU.

**NOTATION**

| | |
|---|---|
| $C$ | Capacity ratio |
| $C_p$ | Specific heat (kJ/kg.K) |
| $D$ | Coil diameter (m) |
| $D_e$ | Equivalent diameter (m) |
| $d_h$ | Hydraulic diameter (m) |
| $d_i$ | Tube diameter (m) |
| $d_{i,inner}$ | Inner diameter of inner tube (m) |
| $d_{i,outer}$ | Outer diameter of inner tube (m) |
| $d_o$ | Annulus diameter (m) |
| $d_{o,inner}$ | Inner diameter of outer tube (m) |
| $d_{o,outer}$ | Outer diameter of outer tube (m) |
| $f$ | Fanning friction factor |
| $f_c$ | Friction factor for curved tube |
| $fs$ | Friction factor for straight tube |
| H | Pitch of the coil (m) |

| | |
|---|---|
| $h$ | Heat transfer coefficient ($W/m^2K$) |
| $k$ | Thermal conductivity (W/m.K) |
| K | Consistency index ($kg/ms^{2-n}$) |
| m | Mass flow rate (kg/hr) |
| n | Power law index |
| $N_{Re}$ | Reynolds number [–] |
| $N_{Re^*}$ | Modified Reynolds number [–] |
| $N_{De}$ | Dean number [–] |
| $N_{He}$ | Helical number [–] |
| $N_{Re,Cr}$ | Critical Reynolds number [–] |
| $T_w$ | Wall temperature (K) |
| UHF | Uniform heat flux |
| $u_o$ | Inlet velocity (m/s) |
| UWT | Uniform wall temperature (K) |

Greek letter

| | |
|---|---|
| $\varepsilon$ | Effectiveness |
| $\Phi$ | Axial angle |
| $\mu$ | Viscosity (kg/m.s) |
| $\rho$ | Density of fluid ($kg/m^3$) |
| $\tau_w$ | Wall shear stress ($N/m^2$) |
| $\delta$ | Curvature ratio (D/d) |

Subscripts

| | |
|---|---|
| $h$ | Hot fluid |
| $c$ | Cold fluid |
| $in$ | Inlet |
| $out$ | Outlet |

## 1. Introduction

Due to compact footprint and higher heat transfer performance, helical coiled-tube heat exchangers demand has been drastically increased in the last few decades. Coiled tube heat exchangers play a key role in heat and mass transfer operations in industrial applications, such as food and chemical process, power generation, heat recovery and refrigeration system, and petroleum, electronics and nuclear industries, etc.[1–14]. The interesting feature of fluid flow in helical coiled-tube is that it can generate the secondary flows by centrifugal forces without having any moving part, which leads to enhancement of heat transfer coefficients[15–17]. In helical coiled-tubes, the fluid in core moves toward the outer wall and then return back to the core due to secondary flow; that generates additional convective current and enhances heat transfer performance[2,6,18–23].

There is an extensive study available in open literature for Newtonian fluids hydrodynamics and heat transfer characteristics in curved pipes[19,23–32]. However, little attention has been paid over non-Newtonian fluid flow and heat transfer in curved pipes. Mishra and Gupta[33] and Mujawar and Rao[20]experimentally studied frictional pressure drop in coiled pipe for both Newtonian and non-Newtonian fluids over a wide range of geometrical parameters (tube diameter, pitch, and Dean number). Hsu and Patankar[34] and Nigam et al.[23] discussed brief outlines of laminar flow heat transfer characteristics for non-Newtonian fluids in curved circular tubes and demonstrated axial and secondary velocity profiles for different power law fluids.

Figueiredo and Raimunda[14], Prasad et al.[5] and Patil et al.[6] reported different design approaches for coil and shell heat exchangers considering helical coils in a shell. It was found that poor circulation was found near the coil in the shell domain, which can be minimized in tube-in-tube helical coil (TTHC) heat exchanger. Mandal and Nigam[35] experimentally studied pressure drop and heat transfer in the TTHC heat exchanger and developed a new correlation for the prediction of friction factor and Nusselt number. Bicalho et al.[36] numerically investigated fluid flow behavior in the concentric and eccentric annuli with/without a rotational inner tube. The fluid-to-fluid heat transfer in annulus and inner tube complicates the design of TTHC heat exchangers, where either heating or cooling is supplied by a secondary fluid, with the two fluids separated by the inner coil wall.

Rennie and Raghavan[37] deliberated the thermal diffusion in a co-axial helical coiled heat exchanger. Two different sized heat exchangers with parallel and counter flow configurations were tested and overall heat transfer coefficients were predicted through Wilson plots. Rennie and Raghavan[31] further numerically predicted heat transfer characteristics in similar configurations for Dean numbers ranging from 38 to 350. The overall heat transfer coefficient variation was found to be in proportional with the inner Dean Number. Whereas, annular flow condition has a high impact on the overall thermal exchange. Further, it was reported that the annular section has more domination in the overall thermal resistance. In another study, Rennie and Raghavan[38] reported non-Newtonian fluid flow in the co-axial helical-coiled heat exchanger with addressing temperature-dependent viscosity. Thermally dependent viscosity has a small effect on the heat transfer phenomena, however, it has a significant influence on the pressure drop.

Reddy[39] numerically predicted the fluid flow and heat transfer behavior in the TTHC heat exchanger taking a wide range of fluid flow rates (400 to 700 *lph*). It was reported that there is around 10% enhancement in the overall heat transfer coefficient by introducing the semi-circular baffles in the annular section. Nada[40] investigated hydrodynamics and thermal characteristics in helical coil heat exchanger considering multi tubes (1-5) in a single helically coiled tube. A correlation has been proposed to predict to Nusselt number taking Reynolds number and number of tubes into account. The effect of the geometrical parameters and operating conditions on the thermal and hydraulic characteristics in the multi tubes-in-tube helical coiled heat exchangers is also reported[41]. The effect of the number of tubes and orientation on thermal diffusion and compactness has been computed numerically.

From the detailed literature, it has been observed that there is very little attention has been paid on the fluid-to-fluid heat transfer considering non-Newtonian fluids in TTHC heat exchanger. The heat transfer study in a TTHC heat exchanger is carried out considering both co- and counter-current flow configurations. In addition to flow configuration, two different geometrical cases of annular section were also considered: 1) with, and 2) without baffles. The fluid flow and heat transfer study in the TTHC heat exchanger is carried out over a wide range of Dean numbers considering the laminar flow regime. The fluid-to-fluid heat transfer characteristics for Newtonian-(inner tube)-to-non-Newtonian (annulus section) and non-Newtonian (annulus section)-to-Newtonian (inner tube) fluids in the TTHC heat exchanger considering baffles in the annulus

section are being reported first time. The fluid flow and heat transfer analysis is carried out in a TTHC heat exchanger for the following configurations:

(i) Countercurrent and co-current flow;

(ii) Newtonian fluid in the inner tube and non-Newtonian fluid (n=0.5, 0.75, 1.0, 1.25) in the annulus section, and non-Newtonian fluid (n=0.5, 0.75, 1.0, 1.25) in the inner tube and Newtonian fluid in the annulus section;

(iii) TTHC heat exchanger with baffles and without baffles.

## 2. Mathematical modelling

The geometrical parameters used in the present study are shown in Table 1. The wall thickness of both tubes was considered about 5% of the outer diameter of the inner tube. The grid size considered was 50 × 200 in radial and axial direction (for single turn), respectively with boundary layers in the vicinity of solid boundaries. Two turns of the helical coil were considered as computational domain to ensure the outflow as fully developed flow at the exit plane. Tube-in-tube helical coiled heat exchanger geometry used in the study has been shown in Figure 1, which also illustrates the adopted grid scheme considering boundary layer attachments to the walls and fine meshing of the computational domain to acquire precise results. The various TTHC heat exchanger configurations considered were:

- Configuration I: Parallel flow with baffles,
- Configuration II: Parallel flow without baffles,
- Configuration III: Counter flow with baffles, and
- Configuration IV: Counter flow without baffles.

The baffles used in the annular section of the TTHC heat exchanger were comprised of semi-circular plates inserted at $90^0$ angles from each other, with alternate flow arrangements, as shown in Figure 1(i). The Dean number was ranged from 50 to 500 for both Newtonian and non-Newtonian fluids. This range of Dean number for both inner and annulus was found in the laminar region as their corresponding Reynold Number is less than the critical Reynolds Number $N_{Re,Cr}$[25] in helical coils:

$$N_{Re,Cr} = 2100[1 + 12(\delta)^{0.5}] \quad (1)$$

**Table 1.**Details of geometrical parameters for TTHC heat exchanger

| Parameter | Inner tube | Outer tube |
|---|---|---|
| Outer diameter (m) | 0.0254 | 0.0508 |
| Inner diameter (m) | 0.023 | 0.0484 |
| Coil diameter (m) | 0.762 | 0.762 |
| Number of turns | 2 | 2 |
| Pitch (m) | 0.1 | 0.1 |
| No. of Baffles | - | 4/turn |
| Baffle C/S area | - | 50% of annulus |
| Baffles thickness (m) | - | 0.0012 |

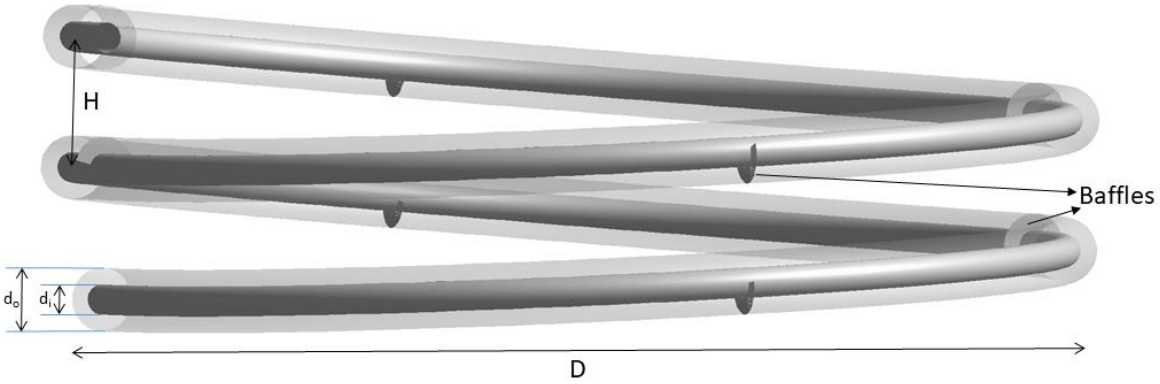


**(i)**

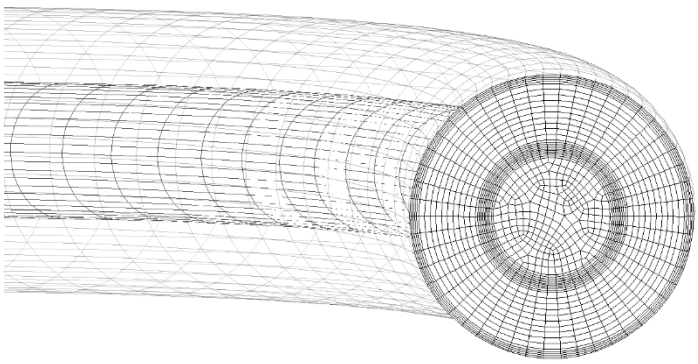

**(ii)**

**Figure 1.** (i) Tube-in-tube helical coil heat exchanger, and (ii) grid topology.

The physical properties such as density, thermal conductivity and specific heat were kept constant for all cases. Steel was used as wall material for tubes with constant properties, i.e. density = 8030 kg/m$^3$, specific heat = 502.48 J/kg-K, and thermal conductivity = 16.27 W/m-K. The Reynolds and Dean numbers were evaluated using equations (2) and (3), as follows:

$$N_{Re} = \frac{\rho u_0 d_h}{\mu} \tag{2}$$

$$N_{De} = N_{Re}(\delta)^{0.5} \tag{3}$$

For the non-Newtonian fluid's Reynolds number, power law equation[31] considering geometrical parameter, power law index and consistency index was used as follows:

$$N_{Re^*} = \frac{\rho {u_0}^{2-n} d_h^n}{K\left[\frac{a+bn}{n}\right]^n 8^{n-1}} \tag{4}$$

$$N_{De^*} = N_{Re^*}(\delta)^{0.5} \tag{5}$$

$$N_{Pr^*} = \frac{\rho^{\frac{(n-1)}{(n-2)}} c_p d_h^{\frac{2(n-1)}{(n-2)}}}{\mu^{\frac{1}{(n-2)}} k} \tag{6}$$

For a circular geometry, the values of $a$ and$b$ are 0.25 and 0.75, respectively. Constant value of consistency index (K) of 0.001 kg/ms$^{2-n}$ was considered in all simulations. The power law index (n) for non-Newtonian fluid was varied from 0.5 to 1.25. The equivalent diameter for the annulus region for heat transfer (Equation 8) and pressure drop (Equation 7) was calculated using the following equations:

$$D_{e,pressure} = \frac{4 \times flow\ area}{wetted\ perimeter} = \frac{4\pi(d_{o,inner}^2 - d_{i,outer}^2)}{4\pi(d_{o,inner} + d_{i,outer})} = \left(d_{o,inner} - d_{i,outer}\right) \tag{7}$$

$$D_{e,heat\ transfer} = \frac{4 \times flow\ area}{wetted\ perimeter} = \frac{4\pi(d_{o,inner}^2 - d_{i,outer}^2)}{4\pi d_{i,outer}} = \frac{(d_{o,inner}^2 - d_{i,outer}^2)}{d_{i,outer}} \tag{8}$$

### 2.1 Governing Equations

In the present study, the Cartesian coordinate system (x, y, z) was used for the computational domain. The governing equations for mass, momentum, and energy for steady-state, incompressible laminar fluid flow considered in TTHC[23] are as follows:

Continuity:

$$\frac{\partial u_j}{\partial x_i} = 0 \tag{9}$$

Momentum:

$$\frac{\partial}{\partial x_j}\left[(\mu_l + \mu_t)\left(\frac{\partial u_i}{\partial x_j} + \frac{\partial u_j}{\partial x_j} - \delta\frac{2}{3}\frac{\partial u_k}{\partial x_k}\right) - \rho u_j u_i - \delta_{ij}P\right] = 0 \tag{10}$$

Energy:

$$\frac{\partial}{\partial x_j}\left[\left(\Gamma_l + \frac{\mu_{tC_p}}{\sigma_\tau}\right)\frac{\partial T}{\partial x_j} - \rho u_j C_P T\right] + \mu_l \Phi_V = 0 \tag{11}$$

where $u_i$ is the velocity component in axial, radial and circumferential directions, $\mu_l$ and $\mu_t$ are laminar and turbulent viscosities, respectively, $\delta_{ij}$ is the Kronecker delta function, and $\mu\Phi_V$ is the viscous heating term in the energy equation, where $\Phi_V$ is given by

$$\Phi_V = \frac{\partial u_i}{\partial x_j}\left(\frac{\partial u_i}{\partial x_j} + \frac{\partial u_j}{\partial x_i} - \frac{2}{3}\mu\frac{\partial u_i}{\partial u_j}\delta_{ij}\right) \tag{12}$$

Shear rate-dependent non-Newtonian viscosity model has been used in the present study. The viscosity for the non-Newtonian fluid is calculated as:

$$\mu = K\dot{\gamma}^{n-1} \tag{13}$$

where $\dot{\gamma}$ is strain rate and k is flow consistency index.

**2.2 Boundary conditions**

The uniform velocity was used at the inlet of both tubes, i.e. $u = U_o$. The hot and cold fluids were defined as non-Newtonian and Newtonian fluids, respectively. At the common boundary between the inner tube and annulus, a coupled heat transfer thermal boundary condition was considered. However, an adiabatic condition was considered at outer wall of the annulus. At the solid surface, no-slip boundary was used (i.e., $u_i$ = 0). The diffusion flux of all variables at the outlet in the exit direction was set to zero as follows:

$$\frac{\partial}{\partial m}(u_i, p, T) = 0 \tag{14}$$

where $m$ is used to represent the normal coordinate direction perpendicular to the outlet plane.

### 2.3 Numerical computation

The governing equations (9–11) were solved using a commercial computational fluid dynamic solver ANSYS FLUENT v16.0.A high order up-winding scheme was used to solve flow and energy equations. Under relaxation factor were taken as 0.3 and 0.7 for pressure and momentum, respectively. The SIMPLEC algorithm was used to resolve the coupling between velocity and pressure components. Convergence criteria for numerical computational convergence were taken as $10^{-5}$ for all the variables.

### 2.4 Grid sensitivity and methodology validation

A grid refinement study was conducted to check the grid sensitivity analysis. Three different cell density (numbers of the cell divided by volume) were modelled and results were compared with Rogers and Mayhew correlation[42] (Figure 2(i)). It is found that the Nusselt number obtained is slightly higher than Rogers and Mahyew[42] correlation, and it may be because of the presence of baffles in the annulus section which creates the boundary layer separation and interlayer mixing that leads to enhancement of the heat transfer characteristics. When the power law index is equal to 1.0 (Newtonian fluids), friction factor predictions were found in good agreement with the data of Mishra and Gupta[33] and Nusselt numbers lies within the range of data provided by Rannie and Raghavan[31], Akiyama and Cheng[26,43] and Mori and Nakayama[44]. This good agreement in the modelling approach can be clearly observed in Figure 2(ii).

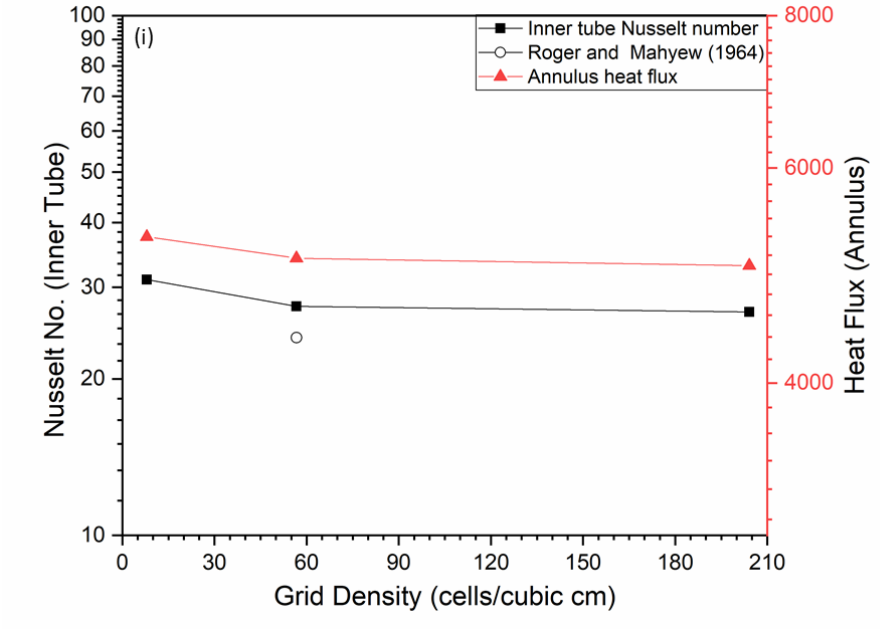


(i)

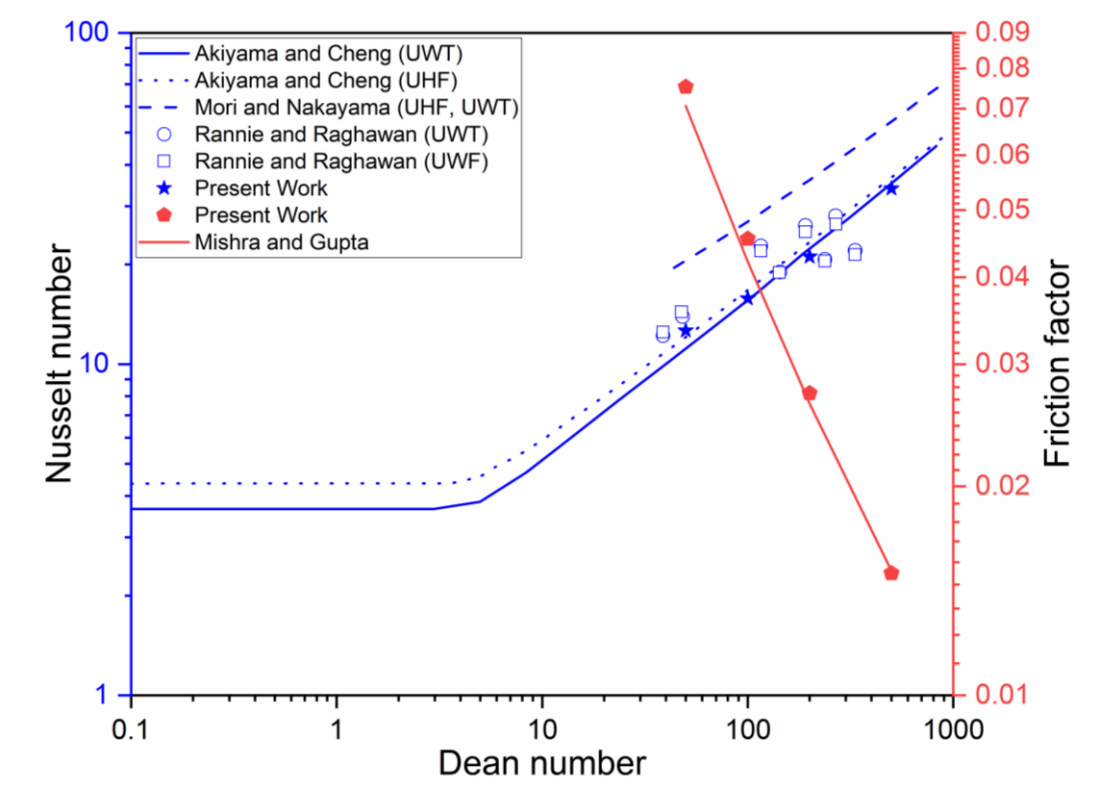


(ii)

**Figure 2.** (i) Grid sensitivity analysis, and (ii) inner Dean number versus inner friction factor and inner Nusselt number.

## 3. Results and discussion

Initially, the effect of the four considered configurations on the heat transfer performance has been tested using four Newtonian fluids (water, cotton oil, ethylene glycol and canola oil). Inlet Dean number, $N_{De}$= 500, was kept constant for both tube and annular fluid zone. The inlet temperature difference between both fluids was taken as 33 in all cases. The thermo-physical properties[45,46] for the considered fluids is reported in Table 2.

**Table 2**. Thermo-physical properties of fluids at 303.15 K.

| Fluid | Heat capacity (J/kg-k) | Density (kg/m$^3$) | Viscosity (kg/m-s) | Thermal Conductivity (W/m-k) | Prandtl Number |
|---|---|---|---|---|---|
| Water[46] | 4182 | 994.65 | 0.00079928 | 0.600 | 5.571 |
| Cotton oil[45] | 2016 | 927.10 | 0.03350400 | 0.613 | 110.222 |
| Ethylene Glycol[46] | 2415 | 1105.60 | 0.01387384 | 0.252 | 132.958 |
| Canola oil[45] | 1904 | 918.30 | 0.06128000 | 0.167 | 698.665 |

It has been seen observed that highly viscous-fluid's viscosity is sensitive towards temperature[47]. Therefore, temperature-dependent viscosity was considered during the simulations. The 5$^{th}$ ordered piecewise-polynomial has been adopted to accommodate temperature in the viscosity function as follow:

$$\mu(T) = A_0T^5 + B_0T^4 + C_0T^3 + D_0T^2 + E_0T^1 + F_0 \quad (15)$$

where $A_0,\ B_0, C_0, D_0, E_0$ and $F_0$ are the coefficients, hence listed in Table 3.

**Table 3.** Coefficients of the piecewise-polynomial for the fluids.

| Fluid | $A_0$ | $B_0$ | $C_0$ | $D_0$ | $E_0$ | $F_0$ |
|---|---|---|---|---|---|---|
| Water | 5.429864250E-14 | -6.813382690E-11 | 2.951343750E-08 | -4.119292120E-06 | -3.566377070E-04 | 1.016589760E-01 |
| Ethylene Glycol | -1.723321000E-11 | 2.969324000E-08 | -2.047593000E-05 | 7.065597000E-03 | -1.220450000E+00 | 8.445864000E+01 |
| Cotton | -2.408653850E-11 | 4.258753610E-08 | -3.015518920E-05 | 1.069094810E-02 | -1.898319410E+00 | 1.351101010E+02 |
| Canola | -4.191025640E-11 | 7.368333830E-08 | -5.188870080E-05 | 1.830107480E-02 | -3.234107160E+00 | 2.292069590E+02 |

All TTHC configurations have been tested over a wide range of operating fluid having different Prandtl number (5.57-698.66). From the numerical analysis, shown in Figure 3, it is found that the design and flow configurations play a significant role in the heat transfer performance. It is also observed that counter flow configuration gives higher performance as compared to the parallel flow configuration. From Figure 3, it can be clearly seen that with an increase in the Prandtl number the heat transfer coefficient increases. Further, at low Prandtl number the baffles have significant influence on heat transfer, while at higher Prandtl number flow configuration has high significance.

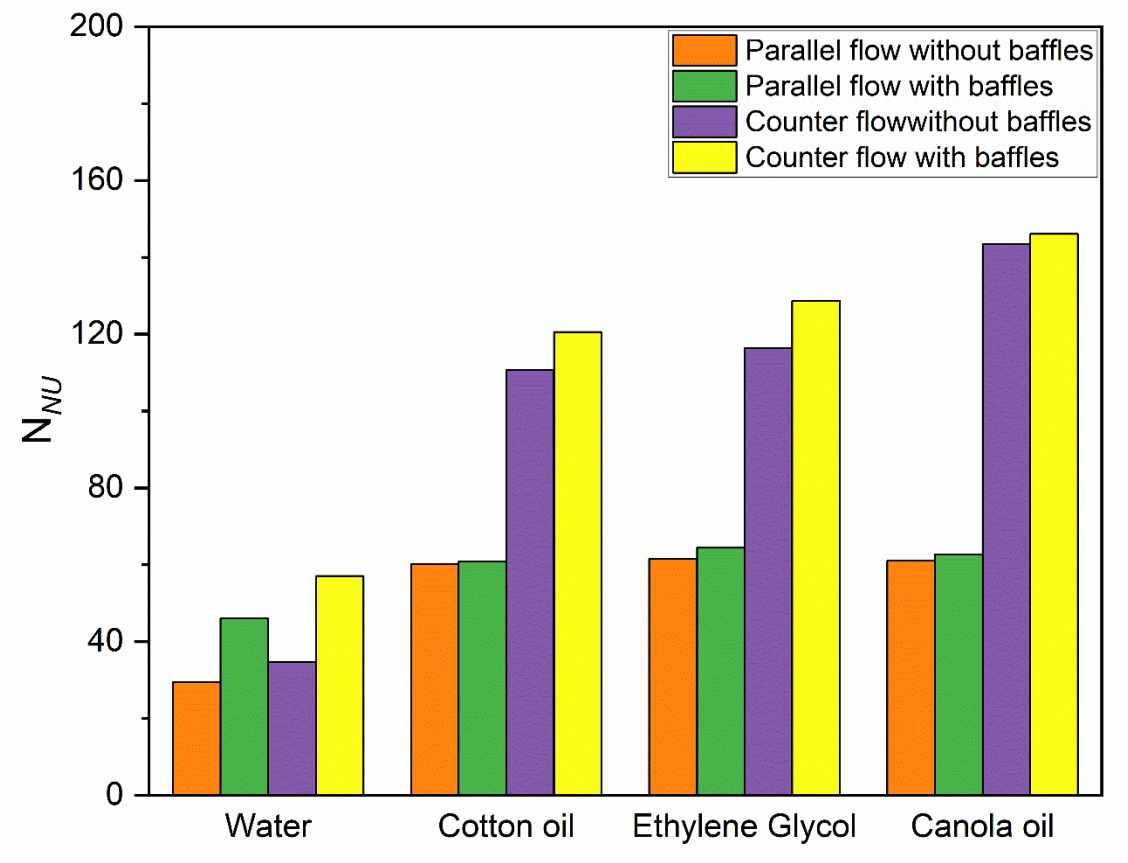


Figure 3. Effect of Prandtl number on Nusselt numberin TTHC with different configurations as well as with and without baffles.

The heat transfers and fluid flow characteristics in a TTHC heat exchanger were analysed using the power law model for both Newtonian and non-Newtonian fluids in various configurations. The velocity contours in the annular section at different axial locations is shown in Figure 4. It can be seen that the presence of baffles in the annular section has a high impact on the velocity profile distribution.

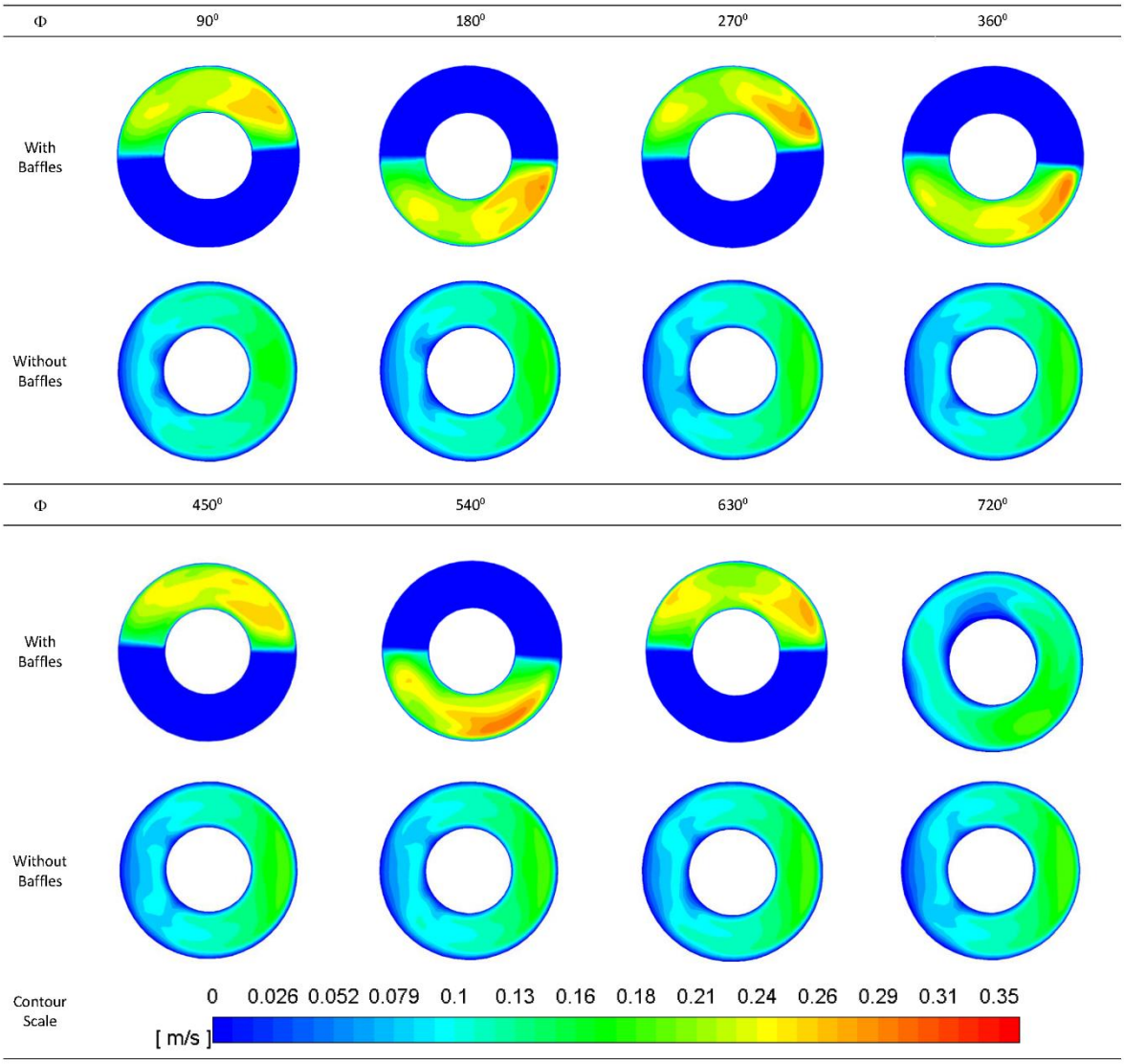


**Figure 4.** Velocity contours of the annular section at different axial locations.

The velocity iso-surface (0.2 m/s) and the path-line in the annular section are shown in Figure 5 for both TTHC designs (with/without baffles). The colours shown in Figure 5, depicts the magnitude of the velocity as per Figure 4 contour scale. Figure 5(i)(a) illustrate the velocity iso-surface in the annular section, which shows the fully developed flow in TTHC without baffles. From path lines of fluids in Figure 5(i)(b), shifting of the maximum velocity towards the outer wall can be easily observed. The chaotic behaviour of the fluid flow in the TTHC with baffles has been illustrated in Figure 5(ii). The baffles creates obstacle in the free flow in the annular section (Figure 5(ii)a) and develop vortex around baffles thus there creates a large variation in velocity distribution (Figure 5(ii)b).

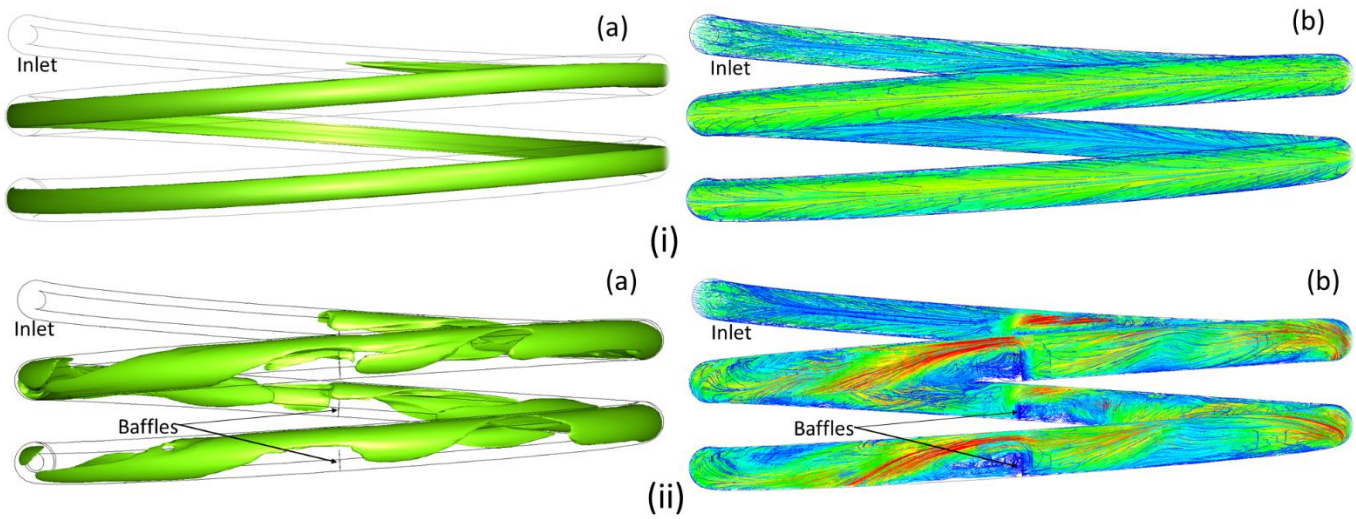


**Figure 5.** Velocity (a) iso-surface and (b) path-lines, in the annular section of TTHC (i) without baffles, and (ii) with baffles.

### 3.1 Friction factor analysis

Friction factor analysis in the TTHC heat exchanger was predicted by the power law relationship for the fluids in the inner tube as well as the annulus region. The Fanning friction factor was calculated as:

$$f = \frac{\tau_w}{\frac{1}{2}\rho u_o^2} \tag{16}$$

where $\tau_w$ is wall shear stress, $\rho$ is fluid density, and $u_o$ is the fluid inlet velocity. The friction factor results for inner tube in TTHC heat exchanger were compared with experimental data of Mishra and Gupta[33], which are represented by the following empirical correlation:

$$\frac{fc}{fs} = 1 + 0.033[log_{10}N_{He}]^4 \;\; for\; 1 < N_{He} < 3000 \tag{17}$$

where $N_{He}$ is the helical number and is represented by

$$N_{He} = \frac{dv\rho}{\mu}\left[\frac{d/D}{1 + (H/3.14D)^2}\right]^{1/2} \tag{18}$$

For laminar flow in the straight tube, the friction factor was calculated using the following equation:

$$f_s = \frac{16}{Re} \tag{19}$$

The friction factors were analysed in the annulus region of the TTHC heat exchanger with different Dean numbers and configurations (annulus with/without baffles). It can be observed from Figure 6, that the friction factor values for the annulus section with baffles are higher than those of the annulus section without baffles because baffles create the boundary layer separation and enhance interlayer mixing which leads to increase in the shear stress. Further, the friction factor predictions are higher for the higher power law index for the same Dean number. For lower Dean number the difference in friction factor predictions for configurations II and IV was 0.2% as compared to the configurations I and III, however, for higher Dean number the difference for friction factor prediction was increased to 19%.

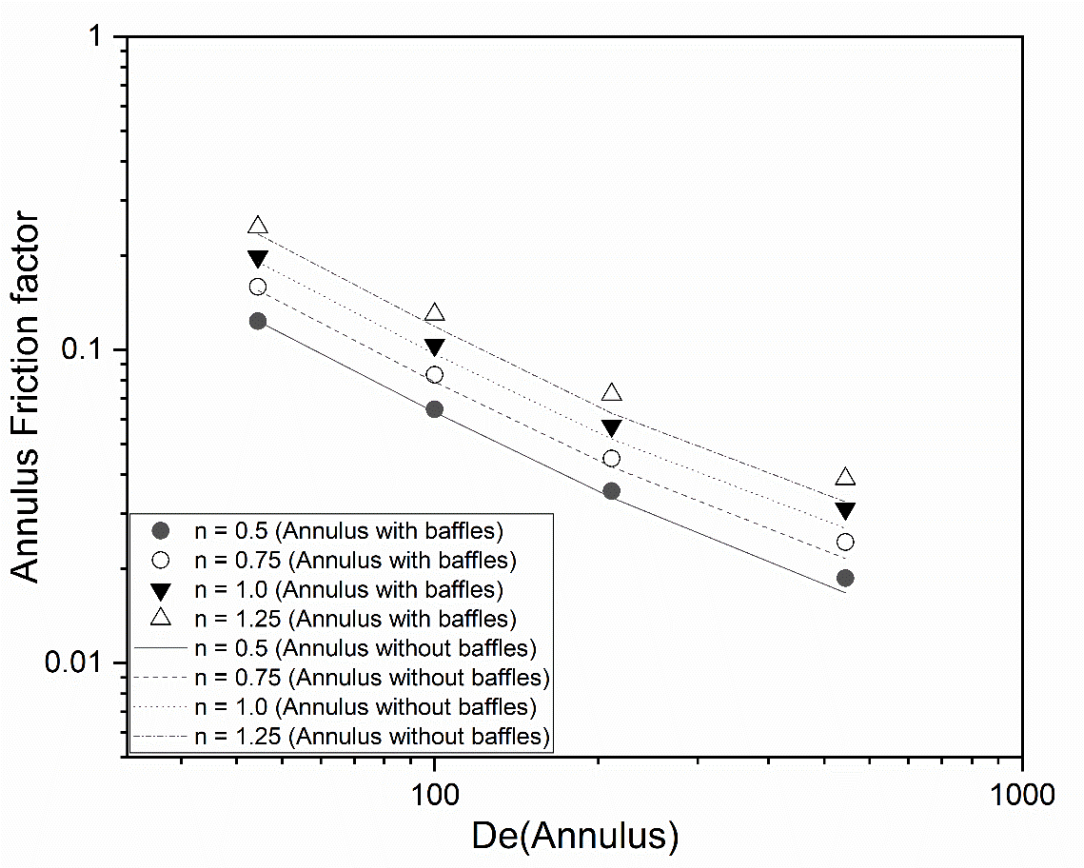


**Figure 6.** Annulus Dean number versus annulus friction factor for power law fluids.

### 3.2 Heat transfer analysis

The heat transfer analysis was made in inner and annulus sections at the fully developed flow region for various configurations of TTHC heat exchangers. The Nusselt number for the inner tube and annulus section was calculated using the following equation:

$$Nu = \frac{h.D_e}{k.(T_b - T_w)} \tag{20}$$

The heat transfer analysis was carried out for the following cases:

- Case I: Hot power law fluids in the inner tube and cold Newtonian fluid in the annulus region.
- Case II: Hot power law fluids in the annulus region and cold Newtonian fluid in the inner tube.

#### 3.2.1 Inner Nusselt number

The variation of the Dean number with the Nusselt number of different power law fluids is shown in Figure 7. The fluid flow pattern was considered as parallel. In the first case, power law fluids were used as the hot fluid in the inner tube and Newtonian fluid was used in the annulus region as a cold fluid. The heat transfer was found slightly higher in the configuration I (with baffles) as compared to the configuration II (without baffles), since the presence of baffles as a bluff body introduce regional mixing in fluid flow area that increases convective heat transfer coefficient.

It can be seen from Figure 7 that the Nusselt number for inner tube increases with an increase in Dean number at the same power law index. This may be due to higher velocity which introduces higher secondary flow. Figure 8 illustrates inner Nusselt number versus Dean number for configurations III and IV, considering power law fluids, inner tube fluid as hot and Newtonian fluid as a cold fluid in annulus region (i.e. case I). Nusselt number values obtained from the counter-current configurations are slightly higher than parallel flow configuration (1% to 8%), which is due to higher log mean temperature difference in case of counter-current configurations. In addition, the Nusselt number values were higher for fluids having a higher power law index at the same Dean number, due to higher secondary flow.

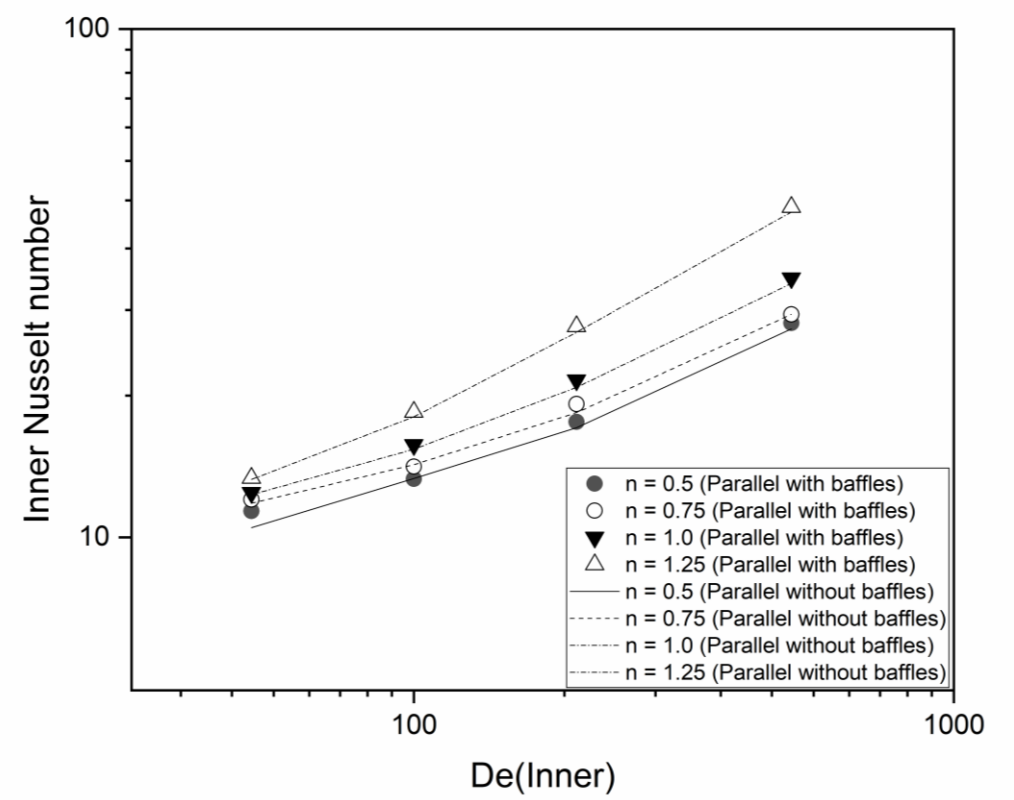


**Figure7.**Inner Dean number versus inner Nusselt number for power law fluids with parallel flow configuration (i.e. configurations I and II).

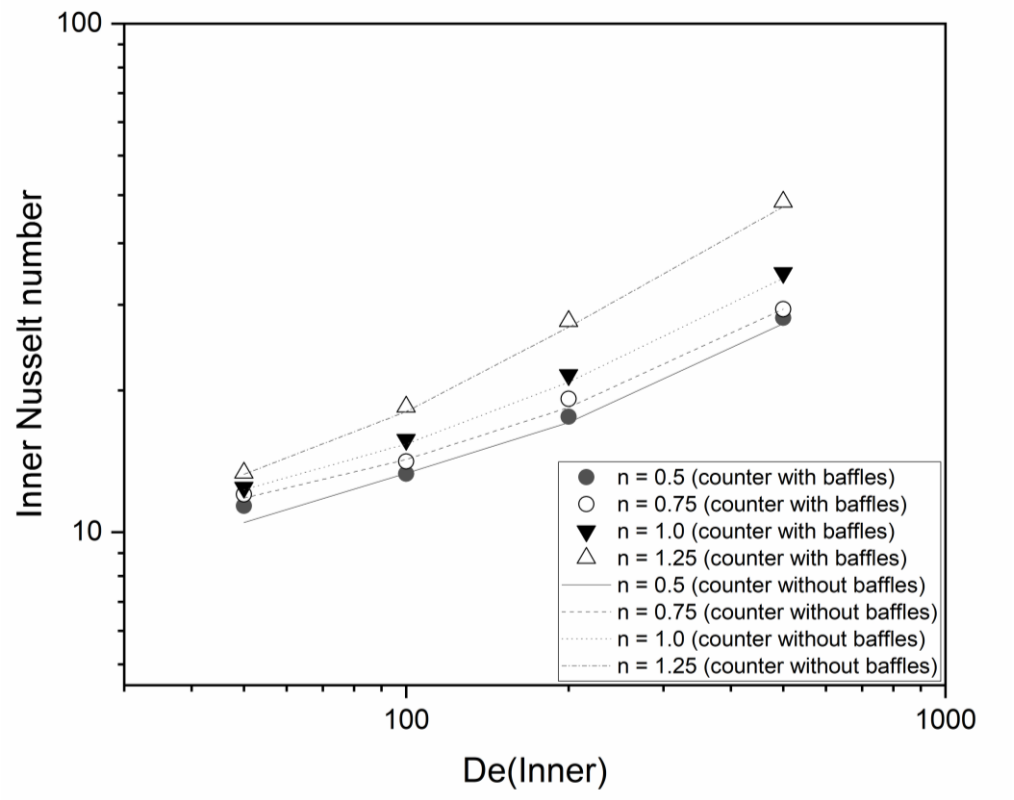


**Figure 8.** Inner Dean number versus Inner Nusselt number for different power law fluids with counter-current flow configuration (i.e. configurations III and IV).

### 3.2.2 Annulus Nusselt number

For this study, the power law fluids were considered in the annulus region while Newtonian fluid was considered in the inner tube (i.e. case II). Figure 9 portray variation of annular Nusselt number with Dean number for different power law fluids for parallel flow configuration (i.e. configurations I and II). It can be seen from Figure 9 that the Nusselt number values are approximately similar for all power law fluids at lower Dean numbers. As the Dean number increases the Nusselt number also increases, with the variation in power law index, which is also in agreement with the results of Nigam et al.[30]. Further, it has been observed that the Nusselt number values for configuration I (i.e. with baffles) are higher as compared to the configuration II (i.e. without baffles), therefore TTHC heat exchangers have more heat transfer when baffles are introduced in the annulus region. It was observed that the difference in Nusselt number variation for configuration I and II was higher at low power law index and lower at high power law index values. The Nusselt number values were approximately 20% higher in case of configuration I as compared to the configuration II.

Figure 10 represents annulus Nusselt number versus annulus Dean number in TTHC heat exchanger with counter-current flow configuration (i.e. configurations III and IV). A similar observation was made as in the case of parallel flow configuration, i.e. the heat transfer coefficient is high when baffles are introduced in TTHC heat exchanger. The presence of baffles in the annulus region creates obstacles in free flow and hence resulted in the high fluid element mixing. The Nusselt number values were ≈14% higher in the case of configuration III as compared to the configuration IV.

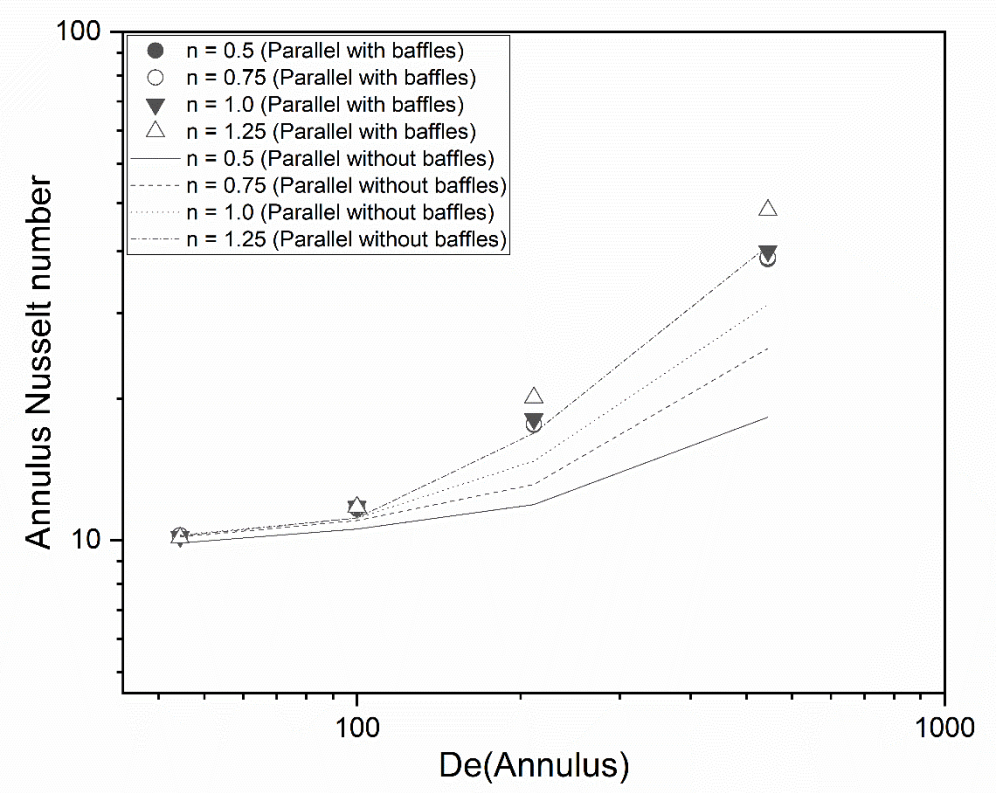


**Figure 9.** Annulus Nusselt number versus Dean number for various power law fluids for parallel fluid flow configuration (i.e. configurations I and II).

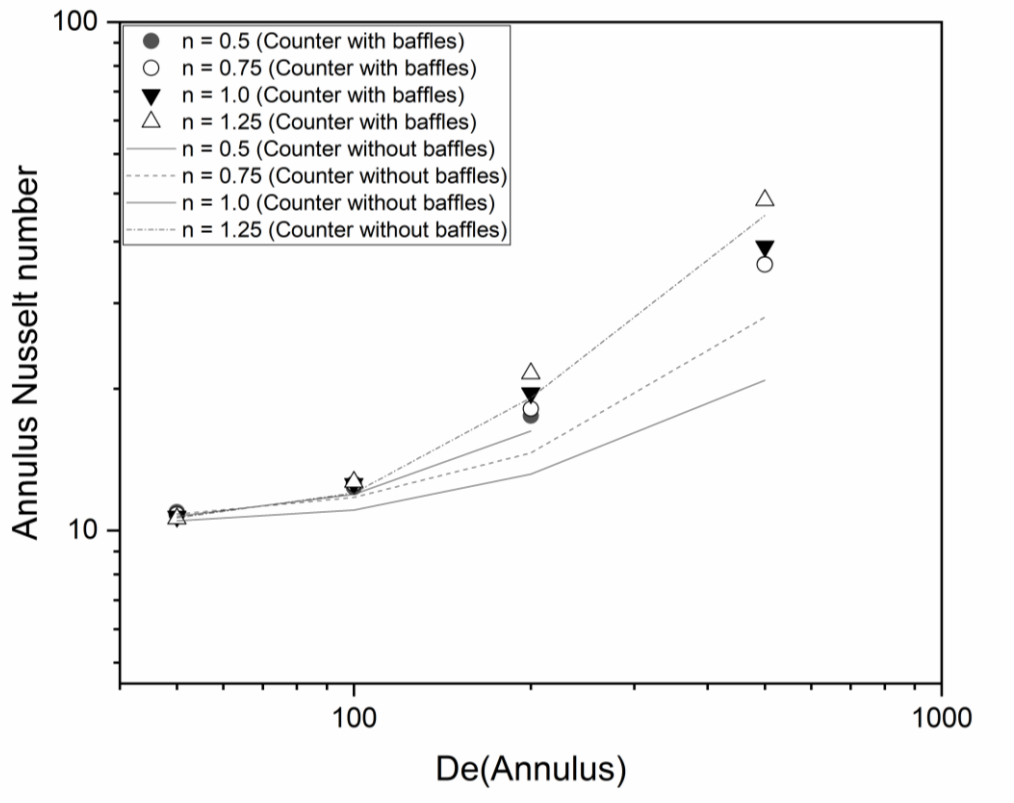


**Figure 10.** Annulus Nusselt number versus Dean number for power law fluids with counter-current configuration (i.e. configurations III and IV).

Further, the heat transfer performance was studied considering the parameter the ratio of Nusselt number with baffles to Nusselt number without baffles, i.e. ($\eta = Nu_{with\ baffles}/Nu_{without\ baffles}$). It is observed (from Supplementary Figure S1) that the value of η varies from 1 to 2 in both flow configurations, i.e. parallel and counter flow, and for less viscous fluids (n = 0.5) the heat transfer perfoamance is higher as compared to the high viscous fluids (n = 1.25). Further, baffles enhances the heat transfer performance of TTHC heat exchanger with factor varying from 1 to 2. For n > 0.75, there is not much increase in the heat transfer performance. A simillar analysis is made for friction factor in annulus considering with and without baffles for different fluids. It is observed that friction factor ratio ($f_{with\ baffles}/f_{without\ baffles}$) increased from 1–1.25 for n varying from 0.5 to 1.25.

The results obtained from the numerical analysis were fitted in the second-order polynomial and power law equation using MATLAB R2019b, and two models have been proposed: 1) generalized, and 2) power law models. Figure 11 shows the good agreement of the obtained data from numerical analysis with the proposed generalized model. The proposed model and coefficient values for considered TTHC configuration has been presented in Equation 21 and Table 4, respectively. In Equation 21 the coefficient $f_1$having small values, however, it can't be ignored as it has more significance in friction factor calculation at higher Dean number.

$$z\,(n, N_{De^*}) = a_1 + b_1(n) + c_1\left(N_{De^*}\right) + d_1(n^2) + e_1(n)\left(N_{De^*}\right) + f_1\left({N_{De^*}}^2\right) \qquad (21)$$

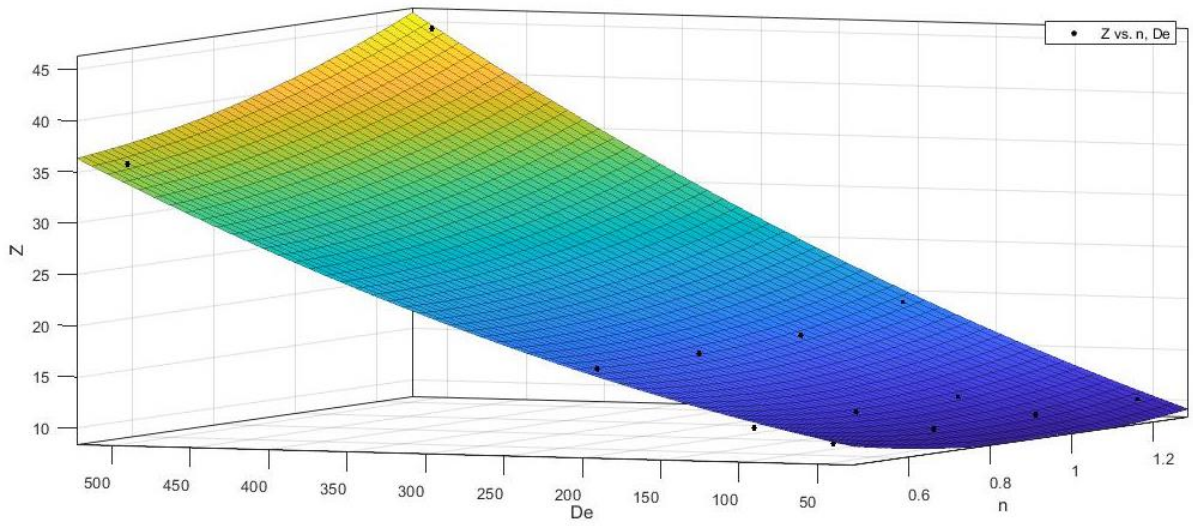


Figure 11. Annular Nusselt number with baffles (parallel configuration) in TTHC.

Table 4: Coefficients values for the proposed model for non-Newtonian fluids (Equation 21).

| $z\ (n, De)$ | $a_1$ | $b_1$ | $c_1$ | $d_1$ | $e_1$ | $f_1$ | $R^2$ |
|---|---|---|---|---|---|---|---|
| *f*(Annular with baffles) | 0.1319 | 0.08307 | -0.001073 | 0.02823 | -0.0002397 | 1.768e-06 | 0.9353 |
| *f* (Annular without baffles) | 0.134 | 0.08052 | -0.001082 | 0.02059 | -0.000218 | 1.759e-06 | 0.9314 |
| *Nu*(Annular without baffles in counter flow) | 15.78 | -10.73 | -0.03608 | 3.443 | 0.06549 | 4.011e-05 | 0.9956 |
| *Nu*(Annular with baffles in counter flow) | 16.85 | -19.23 | 0.01466 | 9.598 | 0.03413 | 2.613e-05 | 0.992 |
| *Nu*(Annular without baffles in parallel flow) | 14.98 | -9.058 | -0.03978 | 2.581 | 0.06111 | 4.402e-05 | 0.9949 |
| *Nu*(Annular with baffles in parallel flow) | 15.64 | -17.35 | 0.01557 | 8.754 | 0.0259 | 4.56e-05 | 0.994 |
| *Nu*(Inner with baffles) | 19.89 | 29.17 | 0.02253 | 17.35 | 0.04622 | -3.112e-05 | 0.9843 |
| *Nu*(Inner without baffles) | 18.65 | -26.44 | 0.0209 | 15.94 | 0.0441 | -2.65e-05 | 0.9843 |

where $a_1, b_1,\ c_1, d_1, e_1$and $f_1$coefficients for generalized model and $R^2$ is regression measure.

The proposed power law model and it's coefficients are shown in Equation 22 and Table 5, respectively. The proposed power law model is a function of the Dean number in case of friction factor, while for heat transfer it is the function of Dean and Prandtl numbers, where Dean number is taking care of inertia and curvature effects and Prandtl number incorporates thermo-physical properties of the fluid.

$$z(N_{De^*}, N_{Pr^*}) = a_2 {N_{De^*}}^{b_2} {N_{Pr^*}}^{c_2} \tag{22}$$

Table 5. Coefficients values for the proposed power law model (Equation22).

| $z(N_{De^*}, N_{Pr^*})$ | $a_2$ | $b_2$ | $c_2$ | $R^2$ |
|---|---|---|---|---|
| *f* (Annular with baffles) | 5.677 | -0.8811 | 0 | 0.8216 |
| *f* (Annular without baffles) | 6.65 | -0.9298 | 0 | 0.8527 |
| *Nu* (Annular without baffles in counter flow) | 0.3556 | 0.5642 | 0.4246 | 0.9097 |
| *Nu* (Annular with baffles in counter flow) | 0.3935 | 0.6496 | 0.2321 | 0.9756 |
| *Nu* (Annular without baffles in parallel flow) | 0.3656 | 0.541 | 0.4303 | 0.8919 |
| *Nu* (Annular with baffles in parallel flow) | 0.3049 | 0.7144 | 0.1803 | 0.9744 |
| *Nu* (Inner with baffles) | 0.5994 | 0.4846 | 0.4675 | 0.947 |
| *Nu* (Inner without baffles) | 0.5909 | 0.4862 | 0.4604 | 0.9363 |

Tables 4 and 5 also report the regression coefficients ($R^2$) for generalised and power law models for the prediction friction factor and Nusselt number in different TTHC configurations, which indicates that the generalized model (Equation 21) predictions for non-Newtonian fluids are applicable for the wide range of the parameters considered in the present work. Further, the Nusselt number and friction factor values from

both models and numerical simulations have been compared in Figure 12. It can be seen that the proposed generalized model better predicts Nusselt number as well as friction factor as compared to the proposed power law model. Therefore, the proposed generalized model is suitable for the prediction of both friction factor as well as heat transfer characteristics in TTHC with different configurations for both Newtonian and non-Newtonian fluids.

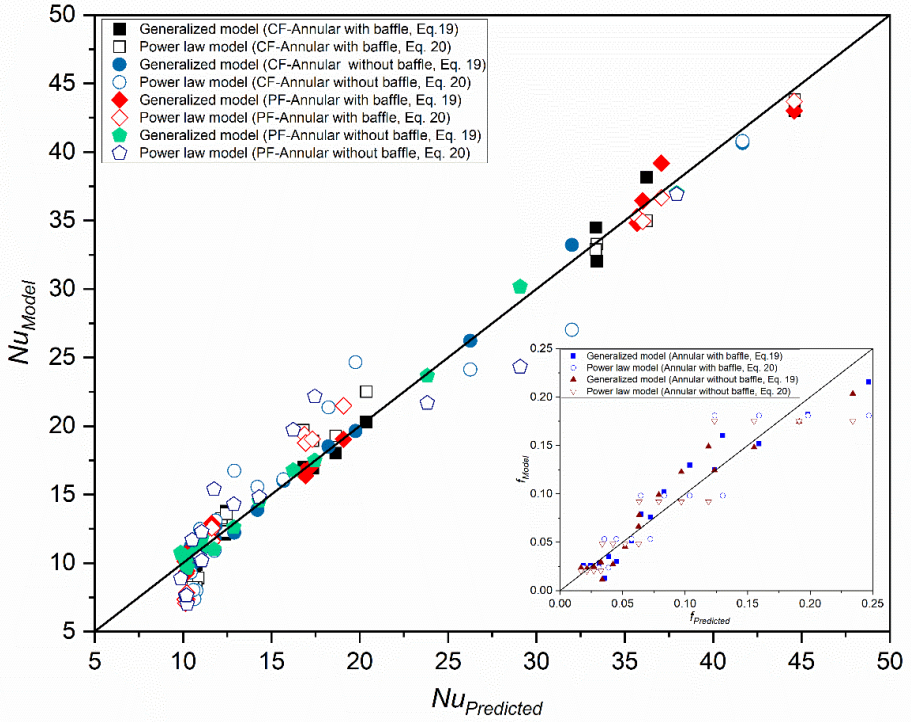


Figure 12. Comparison between predicted data and proposed models (CF–counter-flow; PF–parallel flow).

### 3.3 Effectiveness-NTU approach

The heat transfer analysis for power law fluids in TTHC heat exchanger is carried out using the effectiveness-NTU (*ε–NTU*) method. This will be helpful for the direct design and implementation of a double pipe helical coil heat exchanger in the process industry for power law fluid applications. The effectiveness of TTHC heat exchanger is calculated using Equation 23,which is defined as the ratio of actual heat transfer to the maximum possible heat transfer:

$$\varepsilon = \frac{Q_{act}}{Q_{max}} = \frac{Actual\ heat\ transfer}{Maximum\ possible\ heat\ transfer} \tag{23}$$

The effectiveness of a heat exchanger varies between 0 and 1. The actual heat transfer is defined as the product of capacity rate (the product of mass and specific heat) and the temperature difference of either fluid:

$$Q_{act} = m_h c_h (t_{h,in} - t_{h,out}) == m_c c_c (t_{c,out} - t_{c,in}) \quad (24)$$

A maximum possible heat transfer rate is achieved if a fluid undergoes temperature changes equal to the maximum temperature difference available, i.e.

$$\begin{bmatrix} Maximum\ temperature \\ difference \end{bmatrix} = \begin{bmatrix} inlet\ temperature\ of \\ hot\ fluid \end{bmatrix} - \begin{bmatrix} inlet\ temperature\ of \\ cold\ fluid \end{bmatrix}$$

$$Q_{max} = c_{min}(t_{h,in} - t_{c,in}) \quad (25)$$

Number of transfer unit (NTU) is defined as given below:

$$NTU = \begin{cases} \dfrac{UA}{m_c c_c} & when\ m_c c_c < m_h c_h \\ \dfrac{UA}{m_h c_h} & when\ m_h c_h < m_c c_c \\ \dfrac{UA}{c_{min}} & \end{cases} \quad (26)$$

where $C_{min}$ is the minimum capacity rate ($m.c_p$), $U$ is the overall heat transfer coefficient and $A$ is the heat transfer area. Since $NTU$ is proportional to area $A$, therefore for specified values of $U$ and $C_{min}$, it gives the value of the heat transfer surface area. Larger $NTU$ corresponds to a larger heat exchanger. For double pipe heat exchanger, the effectiveness was calculated using the following equations:

Parallel flow:
$$\varepsilon = \frac{1 - exp[-NTU(1 + C)]}{1 + C} \quad (27)$$

Counter flow:
$$\varepsilon = \frac{1 - exp[-NTU(1 - C)]}{1 - Cexp[-NTU(1 - C)]} \quad (28)$$

where C is the capacity ratio and is defined as the ratio of minimum capacity rate to the maximum capacity rate of fluids (i.e. $C_{min}/C_{max}$).

### 3.3.1 Effectiveness-NTU analysis for case I

Figure 13 shows the variation of effectiveness with the number of transfer units (NTU) in configurations I and II. It can be seen from Figure 13 that the effectiveness increases rapidly at small values of NTU (up to about 2) however, its rate of increasing decreases gradually. The heat exchanger with large NTU values corresponds to a larger surface area and comparatively smaller effectiveness values. Further from Figure 13, it can be observed that the effectiveness values were higher for configuration I as compared to the configuration II. The effectiveness values obtained from numerical calculations were compared with the values obtained from analytical expression for parallel fluid flow configuration (Equation 27). The present predictions for effectiveness variation with NTU are in good agreement with the effectiveness values obtained using analytical expression (Equation 27).

Figure 14 depicts that the effectiveness values obtained for configuration III were higher as compared to the configuration IV. The present predictions for effectiveness variation with NTU were compared with the analytical expression for counter-current flow configuration (Equation 28) and results were found in good agreement. Further higher effectiveness values were obtained for configurations III and IV as compared to the configurations I and II, for the similar NTU values.

### 3.3.2 Effectiveness-NTU analysis for case 2

The variation in effectiveness values with NTU for configurations I and II is represented in Figure 14 and for configurations III and IV is shown in Figure 16. From Figure 15 it can be easily noticeable that the effectiveness values are higher in case of parallel flow configurations with baffles (configuration I) as compared to configuration II (without baffles) for any specified NTU value. Figure 16 shows that for the specified value of NTU the effectiveness is higher in the case of TTHC heat exchanger configuration III (with baffles) as compared to configuration IV (without baffles). Further in counter-current configuration, the effectiveness value at any specific values of NTU was higher as compared to the parallel flow configuration.

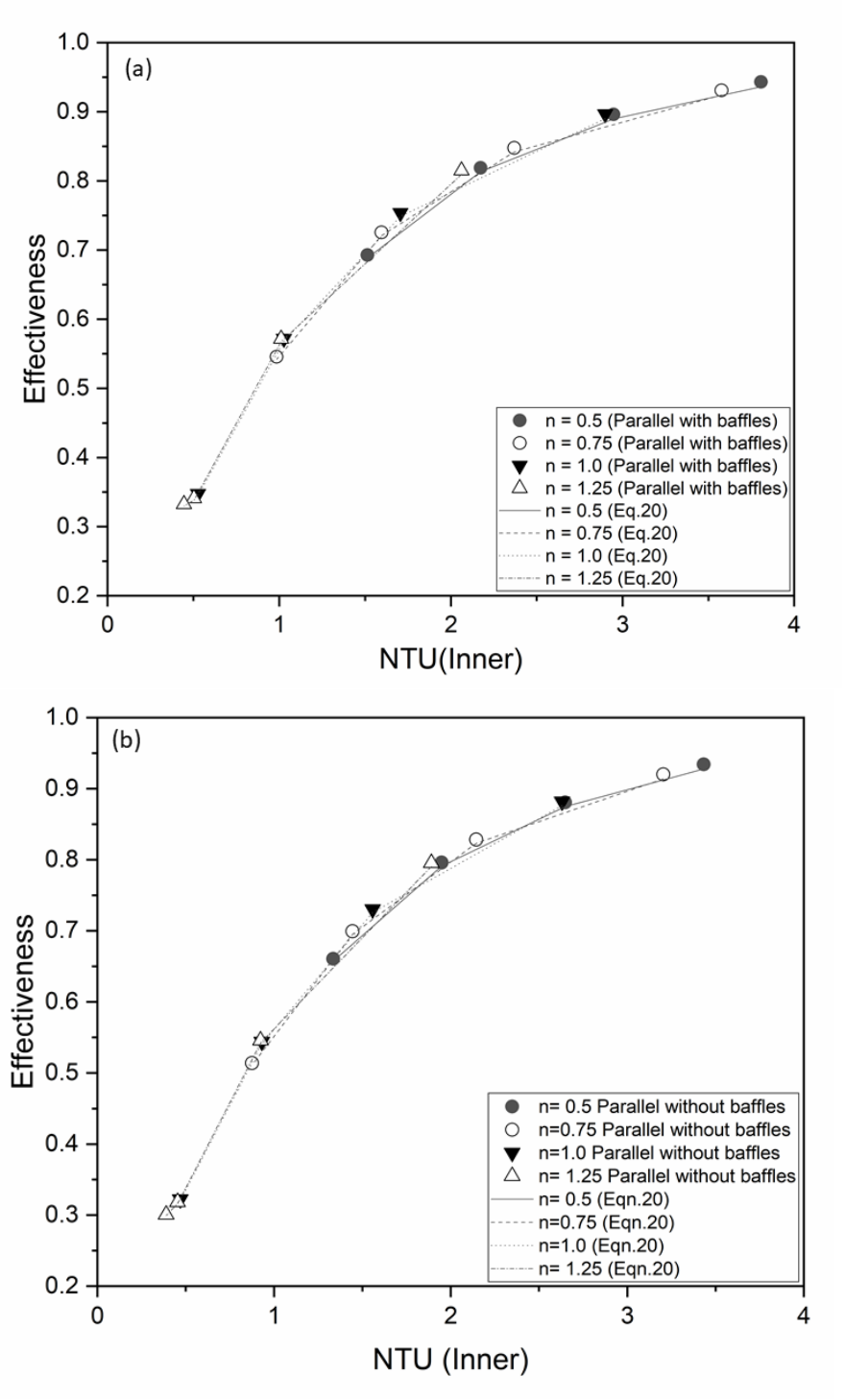


**Figure 13.** Inner effectiveness versus NTU analysis for power law fluids for (a) parallel flow with baffles (configuration I), and (b) parallel flow without baffles (configuration II).

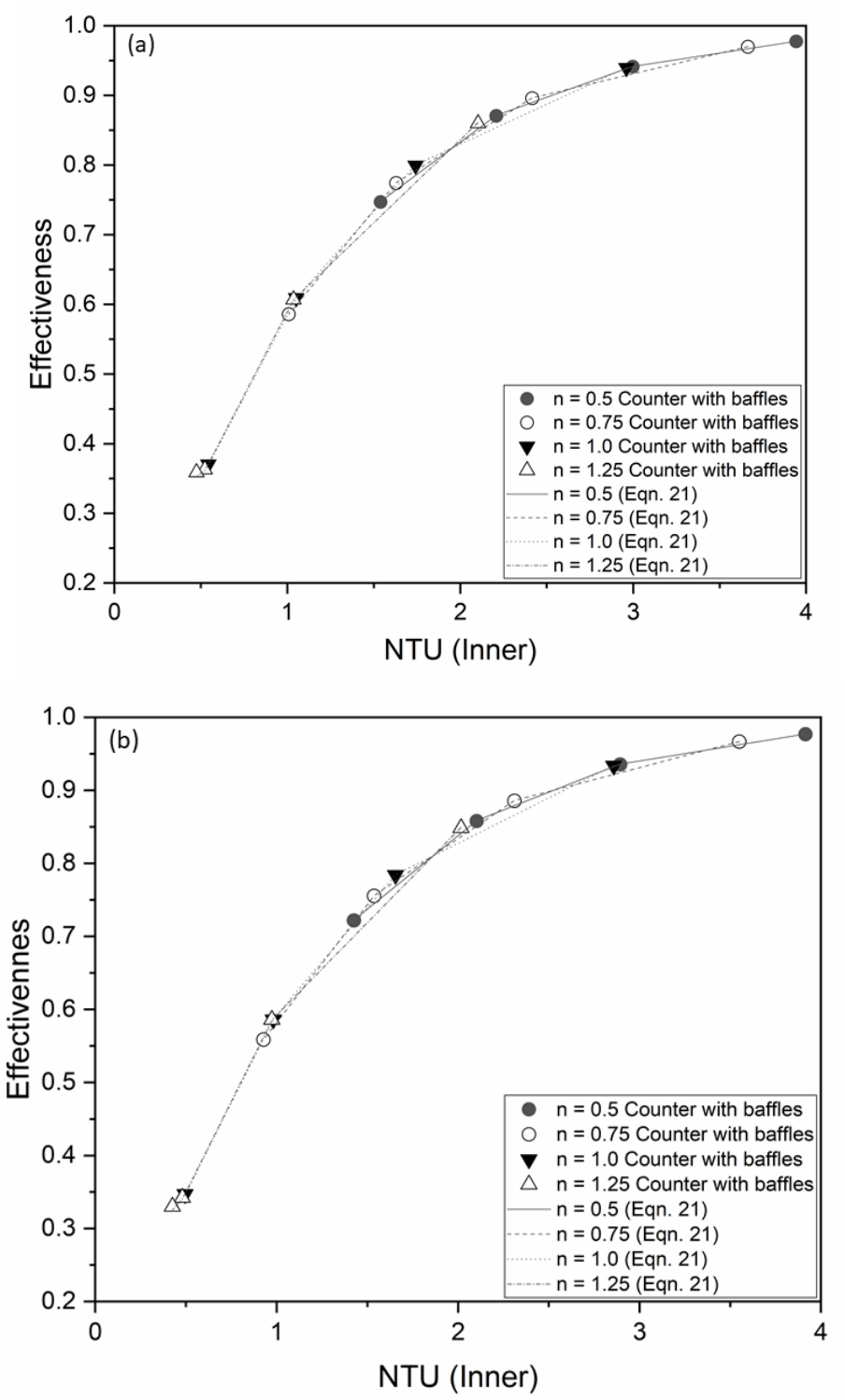


**Figure 14.** Inner effectiveness versus NTU for power law fluids for (a) counter flow with baffles (configuration III), and (b) counter flow without baffles (configuration IV).

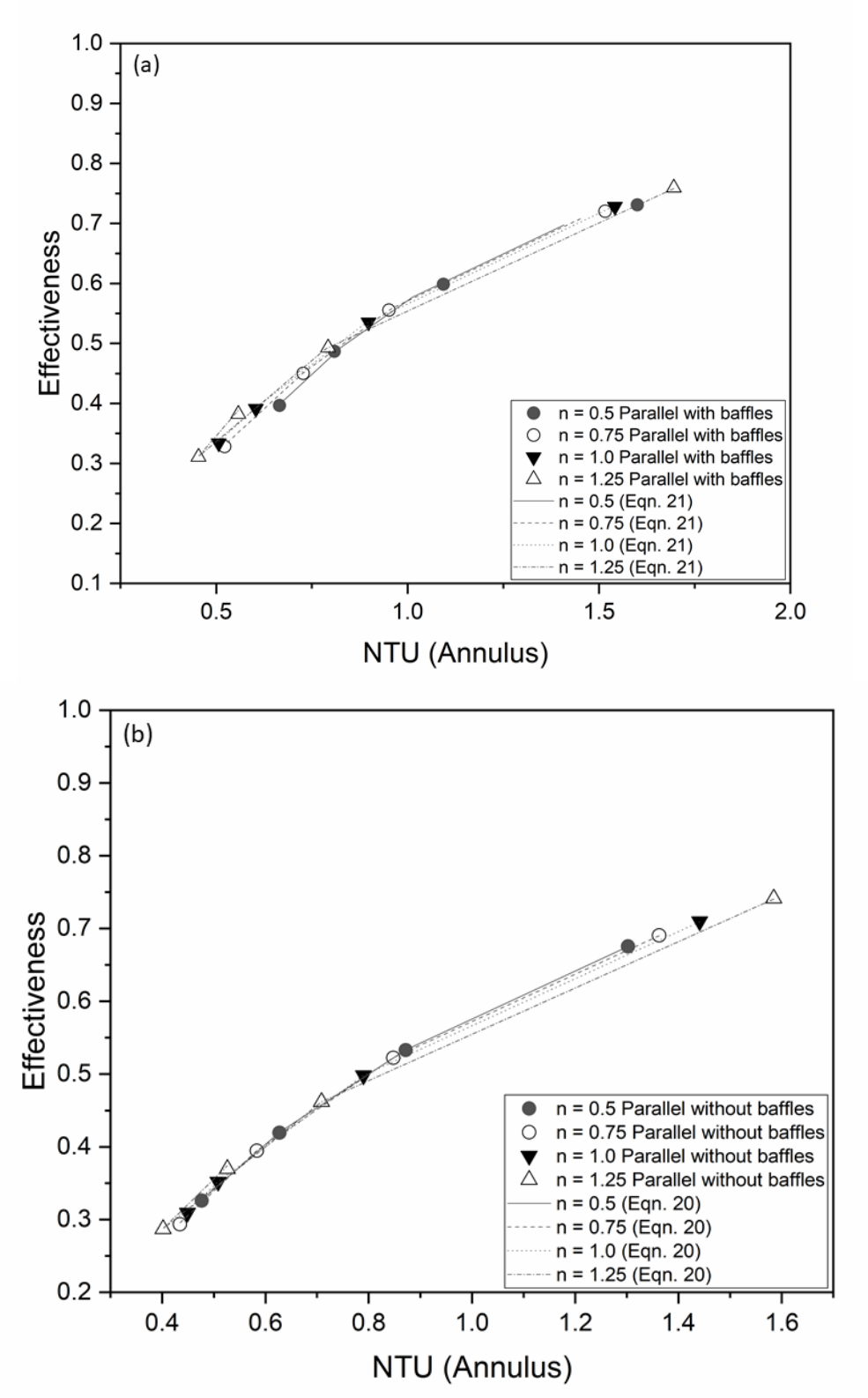


**Figure 15.** Annulus effectiveness versus NTU analysis for power law fluids for (a) parallel flow with baffles (configuration I), and (b) parallel flow without baffles (configuration II).

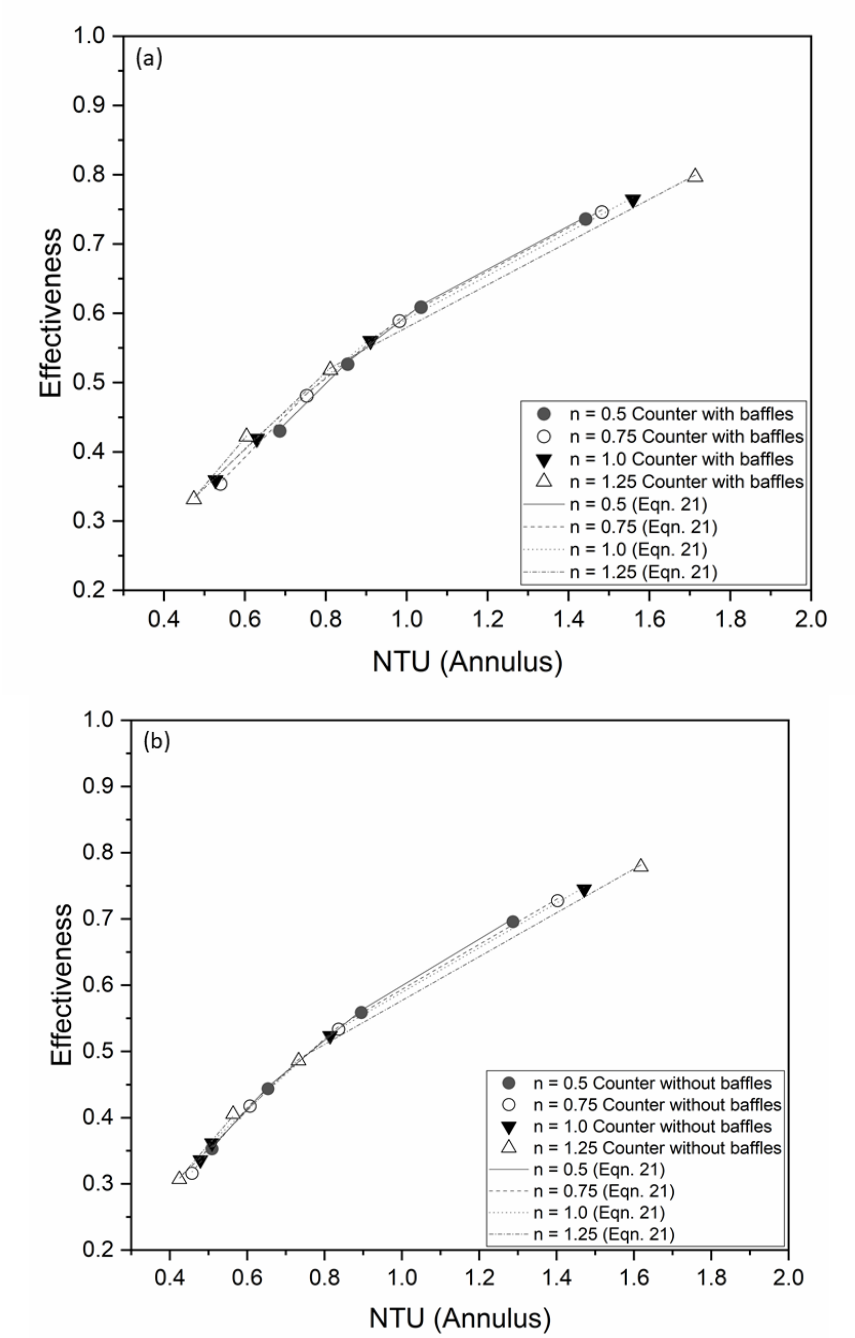


**Figure 16.** Annulus effectiveness versus NTU for power law fluids for (a) counter flow with baffles (configuration III), and (b) counter flow without baffles (configuration IV).

## 4. Conclusions

The key characteristics of the helical coiled-tube is creating the centrifugal forces without having any moving part. These centrifugal forces lead to develop secondary flow which therefore increases the heat transfer rate in the TTHC heat exchangers. In the present work, a numerical study was carried out to predict the friction factor and heat transfer characteristics in the TTHC heat exchanger for Newtonian as well as non-Newtonian fluids with different counter- and parallel- flow configurations. Generalized observation for the configurations are:

1) At lower Prandtl numbers, design configuration (with/without baffles) has more importance over the flow configurations
2) At higher Prandtl numbers, the flow configuration (counter/parallel) has more dominance over design configuration.

The influence of baffles on heat transfer and friction factor characteristics was studied for both the inner and annulus sections of the TTHC heat exchanger. The heat transfer analysis was carried out for two cases.

(i) hot power law fluids in the inner tube and cold Newtonian fluid in the annulus region, and

(ii) hot power law fluids in the annulus region and cold Newtonian fluid in the inner tube.

It was found that the heat transfer enhancement was higher in the case of the TTHC heat exchanger with baffles as compared to the TTHC without baffles. The pressure drop become more due to more shear stress when baffles were employed in the annular section of TTHC. From the obtained results for non-Newtonian fluids with both geometries configurations, i.e. with and without baffles, it was observed that the friction factor decreased with an increase in Dean Number. It can be concluded that for both friction factor and heat transfer the values are higher for fluid having a higher power law index. Two distinct models for the prediction of friction factor and Nusselt number with different configuration have been developed, i.e. generalized and power law models. The results from the generalized model for the Nusselt number found to be very close to the present numerical prediction. Effectiveness-NTU analyses were in very good agreement with the analytical predictions. It was observed that for TTHC with baffles the values of effectiveness were higher for any specified value of NTU and effectiveness values were higher for counter-current configuration as compared to the parallel flow configuration. Therefore, it can be concluded that the higher heat transfer and compactness in geometry makes tube-in-tube helical coil (TTHC) heat exchanger more favourable for heat exchanger applications in the process industries.

**Acknowledgements**

The authors would like to acknowledge the financial support provided by the Ministry of Human Resources and Development (MHRD), Government of India for carrying out the present work.

**References**


(1) Jeong, Y. S.; Kim, J. Y.; Bang, I. C. Enhanced Heat Transfer and Reduced Pressure Loss with U-Pattern of Helical Wire Spacer Arrangement for Liquid Metal Cooled-Fast Reactor Fuel Assembly. *Ann. Nucl. Energy* **2020**, *135*, 106971.

(2) Kushwaha, N.; Vikash; Kumar, V. Impact of Mixed Convective and Radiative Heat Transfer in Spiral-Coiled Tubes. *J. Heat Transfer* **2019**, *141* (8), 1–10.

(3) Xin, R. C.; Awwad, A.; Dong, Z. F.; Ebadian, M. A.; Soliman, H. M. An Investigation and Comparative Study of the Pressure Drop in Air-Water Two-Phase Flow in Vertical Helicoidal Pipes. *Int. J. Heat Mass Transf.* **1996**, *39* (4), 735–743.

(4) Abdalla, M. A. A Four-Region, Moving-Boundary Model of a Once-Through, Helical-Coil Steam Generator. **1994**, *21* (9), 541–562.

(5) Prasad, B. V. S. S. S.; Das, D. H.; Prabhakar, A. K. Pressure Drop, Heat Transfer and Performance of a Helically Coiled Tubular Exchanger. *Heat Recover. Syst. CHP* **1989**, *9* (3), 249–256.

(6) Patil, R. K.; Shende, B. W.; Ghosh, P. K. Designing a Helical-Coil Heat Exchanger. **1982**, 85–88.

(7) Soni, S.; Sharma, L.; Meena, P.; Roy, S.; Nigam, K. D. P. Compact Coiled Flow Inverter for Process Intensification. *Chem. Eng. Sci.* **2019**, *193*, 312–324.

(8) Javadi, H.; Mousavi Ajarostaghi, S. S.; Pourfallah, M.; Zaboli, M. Performance Analysis of Helical Ground Heat Exchangers with Different Configurations. *Appl. Therm. Eng.* **2019**, *154*, 24–36.

(9) Koyun, T.; Jumaah, O. M. Effect of Conic Baffles in the Shell and Helical Tube Heat Exchangers. *Energy Environ.* **2019**, *30* (8), 1437–1455.

(10) Khot, P.; Mansour, M.; Thévenin, D.; Nigam, K. D. P.; Zähringer, K. Improving the Mixing Characteristics of Coiled Configurations by Early Flow Inversion. *Chem. Eng. Res. Des.* **2019**, *146*, 324–335.

(11) Ghobadi, M.; Muzychka, Y. S. A Review of Heat Transfer and Pressure Drop Correlations for Laminar Flow in Curved Circular Ducts. *Heat Transf. Eng.* **2016**, *37* (10), 815–839.

(12) Vashisth, S.; Kumar, V.; Nigam, K. D. P. A Review on the Potential Applications of Curved Geometries in Process Industry. *Ind. Eng. Chem. Res.* **2008**, *47* (10), 3291–3337.

(13) Kumar, V.; Nigam, K. D. P. Numerical Simulation of Steady Flow Fields in Coiled Flow Inverter. *Int. J. Heat Mass Transf.* **2005**, *48* (23–24), 4811–4828.

(14) Figueiredo, A. R.; Raimundo, A. M. Analysis of the Performances of Heat Exchangers Used in Hot-Water Stores. *Appl. Therm. Eng.* **1996**, *16* (7), 605–611.

(15) Dean, W. R. Note on the Motion of Fluid in a Curved Pipe. *London, Edinburgh, Dublin Philos. Mag. J. Sci.* **1927**, *4* (20), 208–223.

(16) Dean, W. R. The Stream-Line Motion of Fluid in a Curved Pipe (Second Paper). *London, Edinburgh, Dublin Philos. Mag. J. Sci.* **1928**, *5* (30), 673–695.

(17) White, C. M. Streamline Flow through Curved Pipes. *Proc. R. Soc. London. Ser. A* **1929**, *123* (792), 645 LP – 663.

(18) Tarbell, J. M.; Samuels, M. R. Momentum and Heat Transfer in Helical Coils. *Chem. Eng. J.* **1973**, *5* (2), 117–127.

(19) Patankar, S. V; Pratap, V. S.; Spalding, D. B. Prediction of Laminar Flow and Heat Transfer in Helically Coiled Pipes. *J. Fluid Mech.* **1974**, *62* (3), 539–551.

(20) Mujawar, B. A.; Roa, M. R. Flow of Non-Newtonian Fluids through Helical Coils. *Ind. Eng. Chem. Process Des. Dev.* **1978**, *17* (1), 22–27.

(21) Jensen, M. K.; Bergles, A. E. Critical Heat Flux in Helically Coiled Tubes. *J. Heat Transfer* **1981**, *103* (4), 660–666.

(22) Kumar, V.; Faizee, B.; Mridha, M.; Nigam, K. D. P. Numerical Studies of a Tube-in-Tube Helically Coiled Heat Exchanger. *Chem. Eng. Process. Process Intensif.* **2008**, *47* (12), 2287–2295.

(23) Kumar, V.; Saini, S.; Sharma, M.; Nigam, K. D. P. Pressure Drop and Heat Transfer Study in Tube-in-Tube Helical Heat Exchanger. *Chem. Eng. Sci.* **2006**, *61* (13), 4403–4416.

(24) Mansour, M.; Liu, Z.; Janiga, G.; Nigam, K. D. P.; Sundmacher, K.; Thévenin, D.; Zähringer, K. Numerical Study of Liquid-Liquid Mixing in Helical Pipes. *Chem. Eng. Sci.* **2017**, *172*, 250–261.

(25) Srinivasan, P. S.; Nandapurkar, S. S.; Holland, F. A. Pressure Drop and Heat Transfer in Coils. *Chem. Eng.* **1968**, CE113-119.

(26) Akiyama, M.; Cheng, K. C. Laminar Forced Convection Heat Transfer in Curved Pipes with Uniform Wall Temperature. *Int. J. Heat Mass Transf.* **1972**, *15* (7), 1426–1431.

(27) Kalb, C. E.; Seader, J. D. Heat and Mass Transfer Phenomena for Viscous Flow in Curved Circular Tubes. *Int. J. Heat Mass Transf.* **1972**, *15* (4), 801–817.

(28) Patankar, S. V; Pratap, V. S.; Spalding, D. B. Prediction of Turbulent Flow in Curved Pipes. *J. Fluid*

*Mech.* **1975**, *67* (3), 583–595.

(29) Karahalios, G. T. Mixed Convection Flow in a Heated Curved Pipe with Core. *Phys. Fluids A* **1990**, *2* (12), 2164–2175.

(30) Nigam, K. D. P.; Agarwal, S.; Srivastava, V. K. Laminar Convection of Non-Newtonian Fluids in the Thermal Entrance Region of Coiled Circular Tubes. *Chem. Eng. J.* **2001**, *84* (3), 223–237.

(31) Rennie, T. J.; Raghavan, V. G. S. Numerical Studies of a Double-Pipe Helical Heat Exchanger. *Appl. Therm. Eng.* **2006**, *26* (11), 1266–1273.

(32) Jayakumar, J. S.; Mahajani, S. M.; Mandal, J. C.; Iyer, K. N.; Vijayan, P. K. CFD Analysis of Single-Phase Flows inside Helically Coiled Tubes. *Comput. Chem. Eng.* **2010**, *34* (4), 430–446.

(33) Mishra, P.; Gupta, S. N. Momentum Transfer in Curved Pipes. 1. Newtonian Fluids. *Ind. Eng. Chem. Process Des. Dev.* **1979**, *18* (1), 130–137.

(34) Hsu, C. F.; Patankar, S. V. Analysis of Laminar Non-Newtonian Flow and Heat Transfer in Curved Tubes. *AIChE J.* **1982**, *28* (4), 610–616.

(35) Mandal, M. M.; Nigam, K. D. P. Experimental Study on Pressure Drop and Heat Transfer of Turbulent Flow in Tube in Tube Helical Heat Exchanger. *Ind. Eng. Chem. Res.* **2009**, *48* (20), 9318–9324.

(36) Bicalho, I. C.; dos Santos, D. B. L.; Ataíde, C. H.; Duarte, C. R. Fluid-Dynamic Behavior of Flow in Partially Obstructed Concentric and Eccentric Annuli with Orbital Motion. *J. Pet. Sci. Eng.* **2016**, *137*, 202–213.

(37) Rennie, T. J.; Raghavan, V. G. S. Experimental Studies of a Double-Pipe Helical Heat Exchanger. *Appl. Therm. Eng.* **2005**, *29*, 919–924.

(38) Rennie, T. J.; Raghavan, G. S. V. Thermally Dependent Viscosity and Non-Newtonian Flow in a Double-Pipe Helical Heat Exchanger. *Appl. Therm. Eng.* **2007**, *27* (5–6), 862–868.

(39) Reddy, K. V. K.; Kumar, B. S. P.; Gugulothu, R.; Anuja, K.; Rao, P. V. CFD Analysis of a Helically Coiled Tube in Tube Heat Exchanger. *Mater. Today Proc.* **2017**, *4* (2), 2341–2349.

(40) Nada, S. A.; Elattar, H. F.; Fouda, A.; Refaey, H. A. Numerical Investigation of Heat Transfer in Annulus Laminar Flow of Multi Tubes-in-Tube Helical Coil. *Heat Mass Transf. und Stoffuebertragung* **2018**, *54* (3), 715–726.

(41) Elattar, H. F.; Fouda, A.; Nada, S. A.; Refaey, H. A.; Al-Zahrani, A. Thermal and Hydraulic Numerical Study for a Novel Multi Tubes in Tube Helically Coiled Heat Exchangers: Effects of

Operating/Geometric Parameters. *Int. J. Therm. Sci.* **2018**, *128* (October 2017), 70–83.

(42) Rogers, G. F. C.; Mayhew, Y. R. Heat Transfer and Pressure Loss in Helically Coiled Tubes with Turbulent Flow. *Int. J. Heat Mass Transf.* **1964**, *7*, 1207–1216.

(43) Akiyama, M.; Cheng, K. C. Graetz Problem in Curved Pipes with Uniform Wall Heat Flux. *Appl. Sci. Res.* **1974**, *29* (1), 401–418.

(44) Mori, Y.; Nakayama, W. Study on Forced Convective Heat Transfer in Curved Pipes : 1st Report, Laminar Region. *Trans. Japan Soc. Mech. Eng.* **1964**, *30* (216), 977–988.

(45) Rojas, E. E. G.; Coimbra, J. S. R.; Telis-Romero, J. Thermophysical Properties of Cotton, Canola, Sunflower and Soybean Oils as a Function of Temperature. *Int. J. Food Prop.* **2013**, *16* (7), 1620–1629.

(46) Bergman, T. L.; Lavine, A. S.; Incropera, F. P.; Dewitt, D. P. *Fundamentals of Heat and Mass Transfer*, 7th ed.; John Wiley & Sons, Inc., 2011.

(47) Kumar, V., Gupta, P., Nigam, K.D. P. Fluid Flow and Heat Transfer in Curved Tubes with Temperature dependent Properties. *Ind. Eng. Chem. Res.* **2007**, *46*, 3226-3236.